Journal of Thermal Analysis and Calorimetry, Vol. 71 (2003) 407–419

IDENTIFICATION OF MICRO-SCALE CALORIMETRIC DEVICES
Part III. The 3-D effects

C. Auguet[1], *J. Lerchner*[2], *V. Torra*[1*] *and G. Wolf*[2]

[1]CIRG-DFA-ETSECCPB, Polytechnical University of Catalonia C/, Gran Capità, s/n,
Campus Nord B-4, E-08034 Barcelona, Spain
[2]Institute of Physical Chemistry, TU Bergakademie Freiberg, Leipziger Str. 29, D-09596
Freiberg/Sachsen, Germany

(Received May 3, 2002; in revised form October 30, 2002)

Abstract

An improved accuracy is researched in flat and silicon based nano-calorimeters related to fluid reaction via drop-to-drop ‘reaction’ or via a steady state in continuous injection of two reactants inside a working chamber. Two types of the experimental aspects of the sensitivity changes, related to 3-D effects, are described: drop effects and volume rate effects. To increase the accuracy, well-controlled Joule measurements are dissipated in the manufacturer resistance and in several resistances in carefully controlled experiments. The shape factor (*SF*) values reduce the manufacturer’s Joule sensitivity up to fifty per cent. A working methodology is proposed: the results are compared with the standard TRIS reaction. The results suggest that the systematic error can be reduced to ±5%.

Keywords: accuracy, chemical nose, conduction calorimeters, identification, liquid mixtures, nano-calorimeters, shape factor, systematic errors, TRIS reaction, working methodology

Introduction

The goal of the actual conduction calorimeters is oriented to progressively miniaturized devices using detector elements with progressively increased sensitivity. The volume reduction is an actual target in all devices (temperature programmed as well as isothermal devices). The miniaturization, an interesting approach, is fuelled by the technological needs of sensitive devices permitting an effective analysis using an extremely reduced quantity of expensive substances.

The technological and the industrial interest is associated to several research domains with reduced available masses. For instance, in organic chemistry and in biochemistry the first synthesis furnishes mass quantities extremely lower that need to be well classified and evaluated. Also, the electronic nose based in an array of calorime-

---

[*] Author for correspondence: E-mail: vtorra@fa.upc.es

1388–6150/2003/ $ 20.00

Akadémiai Kiadó, Budapest
Kluwer Academic Publishers, Dordrecht

ters and via host–guest reactions [1], induces innovative applications in effluent detection (as in pollution detection) or, for instance, in eventual new possibilities via smart systems (or ‘adaptronic’ devices) used in automated capture of fruits as peaches or strawberries. See, for a general overview in smart systems [2].

Manufactured by XENSOR, the liquid nano-calorimeter is one of the available sensors on the market [3]. Mounting the element in an appropriate box the system works as a non-differential calorimetric sensor in, for instance, isothermal condition [4]. Basically the device, with appropriate covers and auxiliary equipment, permits two different groups of measurements – static and dynamic. The static group (null flow rates) relates the reaction between drops: the interest centers on the integral heat of reaction. A careful analysis of the classical parasitic effects as vaporization rate and surface energy joint to 3-D effects related to transported and detected heat is absolutely necessary. The drop reaction is a transient phenomenon. Induces a transitory dissipation associate to the progressive and spontaneous ‘reaction’ between the two drops.

The dynamic group of measurement (associated to flow rates in steady states) visualizes processes with mass flows and relates two types of measurements [5–7]. The first one corresponds to continuous reaction in a liquid mixture by the input of the two components at appropriate rates[**]. In steady state, the enthalpy of mixing is proportional to the output signal. Obviously, the reliability of the measurement depends on the parasitic effects related to the reaction (complete or partial) and to the energy losses related to the mass flow. The accuracy increases if the parasitic effects can be satisfactory corrected. The electronic or chemical nose is the last type of measurement. The analyzed process relates the gas–solid interaction via a host–guest reaction. A flat deposition of one of the reactants (the host) and a gas flow passing from inlet to outlet and containing the other reactant (the guest) permits the gas–solid reaction. The effects, related to the geometrical position of the heat source, can be estimated using the Fourier equation of heat transfer via, for instance, a 2-D representation [8–9]. The gas flow induces two relevant parasitic effects. The first one, the action of the inflow gas, entering at the inlet temperature produces changes on the temperature change created by the reaction. The second one, the outflow gas produces losses in heat and reactants. A part of the produced energy is removed by the gas and, also, only reacts a part of the active substance (or guest) carried by the gas [10].

The volume reduction and the Si-deposition methods creates some auxiliary problems related to heat flux detector. The chip design furnishes a working flat surface appropriate for direct solid–gas reactions or auxiliary miniaturized chambers and/or working micro-devices. Also, the chip is highly sensitive and produces measurable signals with minor thermal power. The main problem, a common problem in the actual devices, relates the heat flux integration. Practically, from the 4πstereo-radians surrounding the sample (an integration ‘sphere’), the covered surface by the detector is practically zero.

[**] In the ‘nano-sized devices’ the available space is extremely reduced, the flows can be considered as laminar and the reaction is realized first and foremost by diffusion.

The extremely lower detecting surface (only a line of 'warmed' thermocouple junctions) is the origin of reproducible but inaccurate results. The flat 'nano-calorimeter' works with excellent resolution and reproducibility but the results are difficult to be compared with Joule measurements using the manufacturer's resistance. A cooperative research program, to improve the accuracy on energy measurements and to establish practical rules for practitioners, is established between the authors. The main axis relates the direct extraction of results from Joule measurements without the use of indirect standard via a comparative reaction or other liquid mixture. In other words, realizing absolute measurement traceable to Joule. The systematic error is 'roughly' expected under 10%. This is the third paper of a cooperative work. In the paper I [11], the shape factor is introduced and the experimental heat positioning effects (heating via a laser spot) on the chip sensitivity are analyzed. In paper II [9], the effects of the heat production are modelled considering the silicon device as a 2-D domain and using the Fourier equation of heat transfer. From the experimental measurements a fit, via the classical Marquardt approach, furnishes the mean values of the physical parameters describing the device. The fitted parameters permit, by simulation, an evaluation of the positioning effects for all heater configurations in 2-D coherent with experimental measurements.

Improvements on accuracy in calorimetric devices need three levels of analysis. The first one, at the classical level of the heat transfer, is related to Fourier equations [12, 15]. The second one, to solve the problems associated to the mass flow and their influence in the produced and in the detected signal. The third one is associated to the chemical reaction level and, in fact, to the true advancement of the reaction.

In this work, two types of the experimental aspects of the sensitivity changes, related to 3-D effects, are described. On the one hand, an experimental test on drop effects is realized. On the other hand, the effects associated to the volume rate in the mixing chamber are studied and the reaction advancement is also considered. An experimental methodological approach is established. The analysis is tested by the TRIS reaction. The gas–solid reaction and the 3-D representation will be treated in subsequent papers.

Experimental

The basic device is a 'non-differential' conduction calorimeter based on the liquid nano-calorimeter LCM 2524 manufactured by XENSOR [3] and silicon based. The working surface is rather thin (25 μm). In the rear, 164 thermocouples of deposited Al and doped Si are located in a frame of squared shape. The device furnishes a working surface close to 1 cm^2 but only in the center (a square of 4×4 mm^2) the sensitivity remains approximately constant (i.e. see papers I and II [9, 11]). The detector direction, determined by the hot and cold junctions, is always practically orthogonal to the heat flows interchanged between the reacting substances and their surroundings. The analysis centers in the positional and in the rate effects using two experimental devices. The first one centered on mixing enthalpy in a 'drop to drop' reaction. The second one, an open device, also centered on mixing enthalpy by a continuous flow of reactants in a mixing chamber.

The noise in the free base line after averaging (*N*), without the parasitic causal effects introduced by bad shielding of pumps and other external devices, is close to 20 μV for a free chip (direct link to digitizing system without preamplifier) and, obviously, sampling and averaging dependent: a mean of repeated measurements reduces the noise. The sensitivity (*S*) using the heater furnished by the manufacturer is close to 2.58 V W^{-1} [11]. The main time constant (τ) is device and contents dependent. In the free surface is close to 0.04 s, and, with working chambers, approaches 10 to 20 s [16]. In drop and in flow-through measurements the signal is pre-amplified. Drop measurements uses a bandwidth of 5 Hz (output sampling period: 0.1 s). In the case of the flow-through device the bandwidth is reduced to 1 Hz (output sampling period: 0.5 s) and the noise does not overcome 0.5 μV (external temperature fluctuations suppressed). From these values the resolution in impulsive signals (established by $N\tau/S$) is roughly situated over 0.3 μJ for free chips and 100 μJ for the drop or the continuous mixture devices. In steady state, the minor power resolution (established by N/S and device type dependent) is situated between 0.2 to 10 μW.

The drops situation

Figure 1 shows an outline of the device with a Pt-resistance (near 11 ohm) situated inside the drop. The thermal contact between the drop and the silicon surface is improved and the wetting process is stabilized via an auxiliary disk (net of cellulose fiber, diameter: 4 mm, thickness: 0.2 mm). The measurements are realized using drops of glycerol (volume 6 and 9 μL), water (9 μL) and undecane (9 μL). The vaporization effect induces perturbations in the measurements. Their effect is determined via the time dependence of the mass. At time close to 30 min, the mass change does not overcome 1% in the used 9 μL water drop. Using a glycerol drop the mass change is not relevant. Eventually a minor increase can be observed related to the water vapor capture. The time scale of the complete Joule measurement is close to 20 min, related to three different steps. The first one, the base line stabilization after mounting (15 min). The second one, a stable output signal associate to a Heaviside Joule signal (2 min) and the third one is the time necessary to recover the base line (2 min). The practical

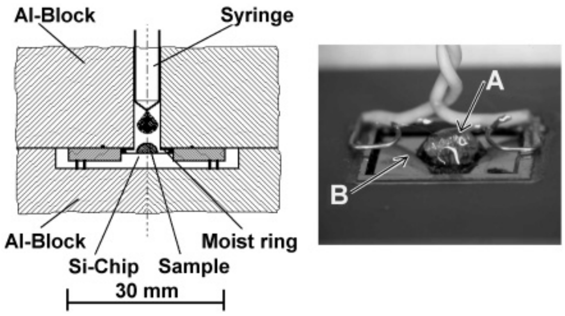

Fig. 1 Left: General outline of the drop calorimeter [4]. Right: photograph of a drop; A – situated in the working surface; B – a 'free' Pt-resistance is situated inside the drop to analyze the positioning effects in comparison with the standard heater furnished by the manufacturer

Joule analysis uses sampling of 0.1 s and several heat pulses (i.e. a series of fifteen on-off signals) to increase the resolution by averaging. After averaging, the available resolution is close to 0.5 μV and equivalent to 0.2 μW.

The continuous injection device

The study of mixtures via continuous injection is realized in the configurations outlined in Fig. 2. A ‘classical chamber’ is outlined in Fig. 2 top. In this study centered on a clearer analysis in the effects of heat transfer and mass flow on the detected signal, two new chambers with different flow path and inserted auxiliary heaters (platinum resistor as in Fig. 3 left) are built. The chamber 1 (Fig. 3 right-top) is a cylindrical hole situated in a plastic element (squared shape) with tubes on the top. In chamber 2, machined to cylindrical shape the upper part, a relevant reduction of the thickness in lateral walls is realized (Fig. 3 right-bottom). The shape of the chamber relates a hybrid structure with cylindrical top and squared bottom.

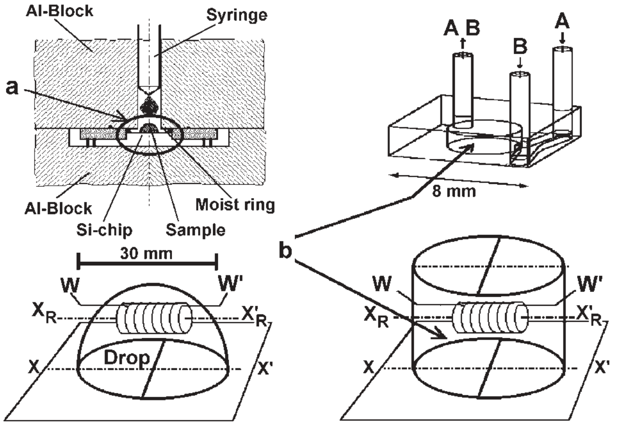

Fig. 2 Top: Schematic outline of the liquid mixtures device [5] with the actual calorimeter (a) and reaction chamber (b). Bottom: enlarged heater position in drops (left) and in chamber (right). Axis of coil heater: $x_R - x'_R$; resistance wire: $W - W'$

Using sampling of 0.5 s, the basic electrical noise in the flow-through configuration is close to 0.5 μV. The noise increases by several causal actions: step motor effects on the injection rate. Also, parasitic couplings between input and output associated to lower coupling impedance can be observed and, eventually, suppressed. Some base line drift actions related to surrounding temperature fluctuation (in particular in the input fluids) can be considered as low frequency noise.

In order to use comparatively chambers 1 and 2 for static (constant mass of liquid without flows) and also for liquid mixtures or chemical reactions, the inlet tube was replaced by a T-shaped one (Fig. 4). The volume of the common path of the reactants, in the inlet tube, is close to 1.4 μL near 7% of the available volume in the chamber (20 μL). The T-shaped inlet facilitates the handling and, from the experimental observations, the

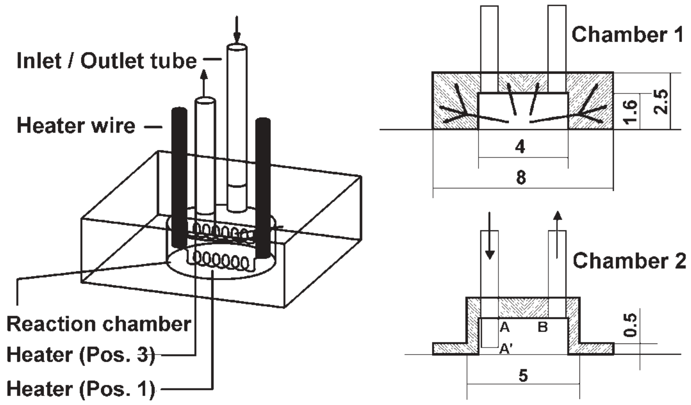

Fig. 3 Left: Liquid flow-through reaction chamber with auxiliary heater at two 'extreme' positions. Right: chamber 1 and 2 (lengths in mm). Top: chamber 1, idealized paths of the heat losses in the cover; some heat losses are addressed to the chip surface in their low sensitivity part [11]. Bottom: chamber 2, outline of the improved device with reduced lateral wall. A–B: low flows inside the reaction volume. A'–B: increased flows improving the mixture via an inflow close to the silicon surface

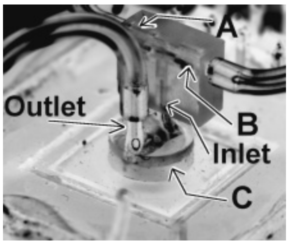

Fig. 4 Reaction chamber with T-shaped mixing tube. A and B: inlets for input fluids. C: working chamber

mixing conditions are improved. The parasitic effects associated to the initial mixing effects inside the T-shaped device and outside the chamber are discussed below.

Results

Three types of experimental results are presented. In the first part, the sensitivity changes on the drop device are evaluated. The second part concerns the *z*-dependence of the sensitivity in different geometry of the flow-through chamber and of the undetected heat via direct heat losses to surrounding by the mass flow. The third part shows some experimental measurements of actual mixtures and the associated thermodynamic formalisms.

In the actual analysis, several Joule effects in different liquids and resistance position are studied. Usually the chip heater (CH furnished by the manufacturer) and three heaters (a coil in platinum wire). The drop device uses drop heater (DH) in low,

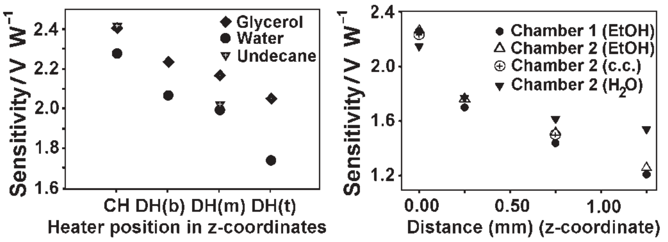

Fig. 5 Left: the *z*-position effects on sensitivity (S) in drops of 9 μL glycerol, water and undecane, respectively, measured using an auxiliary heater inside the drop (DH – drop heater). The zero position relates the manufacturer's resistance (CH – chip heater). Right: the *z*-position effects on sensitivity (S) in a flow-through chamber for ethanol and water. The zero position relates the manufacturer's resistance (chip heater). The chamber 1 data are associated to liquid injection on top [11]. In chamber 2 the injection is close to the silicon surface. See, in Fig. 3 the appropriate shapes. Chamber 2 (c.c.) means cut corners

central and upper (or high) position. The chamber system is also mounted in three *z*-positions in three 'identical' devices. For instance, Fig. 5 left shows the sensitivity dependence on drops and Fig. 5 right shows the *z*-effects for the mixing chamber. In Fig. 5 right, full dots correspond to the preliminary *z*-sensitivity effects presented in paper I of this series [11]. The platinum coil resistor has a cylindrical shape (length close to 3 mm and diameter near 0.4 mm). The cylinder mainly produces heat in only one privileged axis (1-D). Using a 2-D simulation the estimated differences between a warmed rectangle with 3×0.6 mm^2 (resistance coil projected to the silicon surface) and the manufacturer's resistance (a squared frame near the warm junctions with 6.8 mm^2) does not overcome 1% [9]. Analyzing Fig. 5 it is evident that sensitivity changes in the chip heater are relatively lower in comparison with the *z*-effects: the chip heater masks the relevant changes related to substance and dissipation position inducing misunderstanding and, eventually, relevant systematic errors.

Drop results and shape factor values

The results of the drop experiments are summarized in Table 1. Repeated measurements with new positioned drops of the same volume of liquid demonstrate a mean reproducibility close to 1%. A remarkable decrease in sensitivity regarding the drop heater results if the volume of the drop is increasing from 6 to 9 μL, whereas the volume change does not influence the sensitivity associated with the chip heater. The change in sensitivity depending on the position of the heater within the drop is shown in Fig. 5 left for water, glycerol and undecane, respectively. As expected, sensitivity depends on the liquid and their value decreases with the distance of the heater to the chip membrane. But it is noteworthy that the sensitivity associated with the water drop is remarkably lower than that of glycerol in the chip heater as well as in the drop heater.

The lower value of the chip heater sensitivity in the case of water seems produced by evaporation effects. In fact, we have measured a mean mass loss of 150 μg h^{-1} with minor supplementary effects related to room temperature oscillations probably inducing changes in the laboratory water vapor pressure. Particular evaporation effects associated to Joule dissipation remain under the detection level and further study seems convenient. In comparison with water, glycerol and undecane have very low vapor pressures but strongly different viscosity. The differences in the drop heater sensitivities at equal positions are additionally influenced by heat conduction to XENSOR chip taken into account by the shape factor.

Table 1 Sensitivities *vs*. drop volume and used liquid for Joule heating using chip heater (S_{CH}) and drop heater (S_{DH}) related to the net-disk effect. Reproducibility analysis: R: complex repeated measurement

No.	Drop type	S_{CH}/V W^{-1}	S_{DH}/V W^{-1}
1	Water, 9 μL, with net-disc	2.286	2.000
2R	"	2.272	1.987
3R	"	2.217	1.990
4	Water, 9 μL, heater in lower position	–	2.070
5	Water, 9 μL, heater in upper position	–	1.743
6	Gylcerol, 6 μL, without net-disc	2.409	2.259
7R	"	2.405	2.270
8R	"	–	2.255
9	Glycerol, 6 μL, with net-disc	–	2.277
10R	"	–	2.271
11	Gylcerol, 9 μL, with net-disc	2.406	2.172
12	Gylcerol, 9 μL, heater in lower position	–	2.238
13	Glycerol, 9 μL, heater in upper position	–	2.053
14	Undecane	2.420	2.027

For water and glycerol, shape factors can be estimated from Fig. 5 left. Assuming an homogeneous dissipation in the complete volume of the drop, the *SF* value are close to 0.889 and 0.896. In drops, the sensitivity changes are liquid dependent with a relevant *z*-dependence. The behaviour is similar when a chamber is used.

An example: the TRIS protonization reaction

Using deposed drops of 3 μL of 50 mmol L^{-1} HCl in the device surface stabilized by the cellulose disc and adding 4.4 μL of 0.1 mol L^{-1} a TRIS reaction*** is produced. The output calorimetric response (or curve) needs to be corrected from relatively re-

---

*** The TRIS reaction is represented by: $C(CH_2OH)_3NH_2+H^+\rightarrow C(CH_2OH)_3NH_3^+$

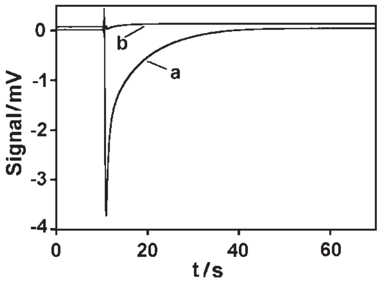

Fig. 6 Signal from a TRIS protonization experiment (a: corrected signal regarding mixing and dilution effects; b: signal due to TRIS dilution

duced dilution effects (in Fig. 6 the TRIS dilution effect). Using a chip sensitivity of 2.33 V W^{-1}, the obtained molar enthalpy is 44.0 kJ mol^{-1} with a resolution of 1 kJ mol^{-1} [17]. This is 7% below the published value of 47.4 kJ mol^{-1} [18]. Applying *SF* of 0.908 established by a mean value of sensitivity for water drop close to 9 μL, a corrected value of 48.5 kJ mol^{-1} is obtained (systematic error range ±2.5%).

Chamber results: liquid effects and the SF values

The preliminary analysis [11, 16] established that the sensitivity values, evaluated by the chip heater and the auxiliary heaters in different positions, are dependent on the size of the chamber and on the thermal properties of the samples. In the chambers used (Fig. 3) the size of the chamber does not induce relevant influence on chip sensitivity, i.e. minor effects appears with changes in the lateral thickness of the chamber and in the suppression of the chamber corners (Fig. 5 right). Also, the effects related to the auxiliary heaters are reduced. From the experimental observation it seems possible to consider that 'not relevant' heat (or, in equivalent situation 'similar but not detectable') is transferred to the silicon surface in their low sensitivity part (heat losses schematised in Fig. 3 right top). Analyzing the sensitivity results regarding chip heater and the auxiliary heaters in different *z*-position the different thermal properties of the used liquid are highly relevant.

Several series of measurements were performed to analyze the reproducibility of the chambers and heaters (i.e. manufacturing, preparation and mounting). The observed deviations were less than 2 per cent. Further, the influence of vertical convection was tested by measuring the sensitivities in a 180° turned position of the device. In general, the chip heater sensitivities are 3 per cent lower in the turned position. On the contrary, the sensitivities regarding the auxiliary heaters are practically equal. For example, using ethanol the values are 1.717 and 1.720 V W^{-1} (normal and reversed position) for the heater situated inside the chamber in the lower position. From the measurements it can be considered the existence of some convection to the surroundings in heat dissipated in the silicon device (close to the rear surface) and undetectable effects in the internal dissipation (heater inside the chamber).

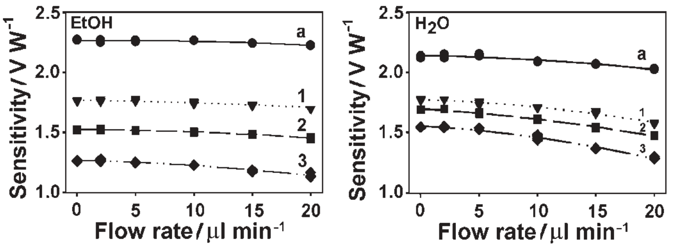

Fig. 7 Positional and rate effects on sensitivity. Left: flow rate effects with water. Right: flow rate effects with ethanol (a – chip heater, 1…3 – auxiliary heaters at positions 0.25, 0.75 and 1.25 mm, respectively, in *z*-axis)

Chamber results: flow rate effects

In the case of chamber 2 (Fig. 3) the flow rate dependence of the sensitivities for all heater positions was studied. Figure 7 indicates that the decrease of the sensitivity due to the mass flow is progressively higher with increasing *z*-axis distance of the heater position to the membrane. At relevant *z*-position the heat is practically undetected: the mass flow transports the heat directly to the outlet. The value at flow rate of 20 μL min^{-1} decreases the sensitivity from 2 to 10% if the chip heater or the heater at top positions are used. As the detected signal is the temperature, the signal decrease also depends on the heat capacity of the sample. As a matter of fact, the measurements establish a decrease of the sensitivity with the increase of volume rate and, at zero rate, remains the heater positioning effect. In homogeneous dissipation and in steady state the parasitic effects related to flow rates and to each different liquid need to be corrected.

A practical approach to SF, volume rate and partial reaction effects

From the measurements associated to a chemical reaction or a mixing enthalpy, five steps need to be considered. The first one relates the particular values of sensitivity for each liquid type. The second one, the expected shape and position of the dissipation in the studied phenomena furnishing the appropriate shape factor *SF*. The third one, the rate effects. The fourth one is a common problem in miniaturized devices: the components travelling inside the chamber without reaction. A suitable protocol need to be built if experimental results are converted to a ‘full reaction’ for appropriate evaluation of thermodynamic parameters. The last one, a thermodynamic formalism adapted to each studied process.

Suggested methodology

a) From the experimental analysis, Joule sensitivity dependence needs to be determined according to the liquids used, i.e. with the final mixtures or products.
b) *SF* needs to be evaluated according to the expected position of the dissipation, i.e. for a hypothetical homogeneous dissipation the *SF* is S_{CH}/S_m (S_{CH} is the chip sensitiv-

ity, S_m the mean z-axis sensitivity). If the dissipation can be associated to particular positions inside the chamber *SF* needs to be modified accordingly.

c) The results of measurements need to be extrapolated to zero rate. In this situation *SF* approach can be applied.

A case of study: the TRIS reaction

As a preliminary test the TRIS reaction [18] is studied working in chamber 2 using the T-shaped inlet mixing chamber (Fig. 4).

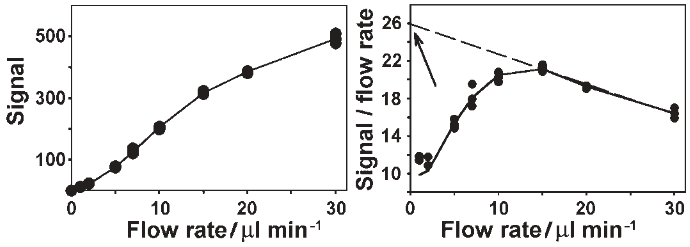

Fig. 8 Left: Signal for the protonization of TRIS (0.1 mol L^{-1} TRIS, 0.02 mol L^{-1} HCl) *vs*. flow rate. Right: Relative signal (signal/flow rate) *vs*. flow rate

The steady state signal *vs*. the flow rate of the TRIS protonization reaction is depicted in Fig. 8 left and the signal divided by the flow rate *vs*. flow rate in Fig. 8 right. From Fig. 8 right it is evident that the extrapolated value (at zero rate) is zero. In other words, at 'zero rate' the reaction is 'realized' in the external T-shaped device. At lower rates (under 10 µL min^{-1}) the part of the injected components which reacts in the 7 mm long common tube increases progressively. The heat loss through the tube increases with decreasing flow rate and therefore the extrapolation to zero flow rate of the derived curve (signal divided by flow rate) furnishes a zero signal.

To establish a protocol for appropriate extrapolation a parallel analysis is realized. Using a colored reaction (i.e. the Fe^{3+}+SCN^{-}) producing an intense red colored complex a progressive decrease of the reaction advancement inside the T-shape (in the 7 mm inlet) is obtained increasing the volume rate. A 'zero' advancement (no reaction inside the inlet) can be considered for volume rates close or higher to 10 µL min^{-1}. With increased volume rate the reaction is realized out of the device, eventually, in the outflow liquid. Extrapolating the last part of the results (only the higher volume rates are used) to zero volume rate their value can be related with a reaction only realized inside the chamber. A simple linear extrapolation using values from 15 µL min^{-1} yields an extrapolated value of 26 µV min^{-1} and the suggested *SF* is the mean value for water (0.79) associated to a homogeneous dissipation inside the chamber. The estimated value for the TRIS reaction enthalpy is 45.8 kJ mol^{-1}. This is a reasonable attempt (3.5 per cent from the value (47.4 kJ mol^{-1}) deduced from reference [18]) because an exact description of the flow rate effects is not yet available now but the value deduced directly form the chip heater is 36.2 kJ mol^{-1} with a difference of 26%.

The thermodynamic formalism

In a binary liquid mixture from pure components 1 and 2, quantities n_1 and n_2 and the molar enthalpy values H_1^* and H_2^* in pure substances and H_1 and H_2 in the mixture, the enthalpy change ΔH_M for one mole of mixture related to the mixture can be written as:

$$(n_1+n_2)\Delta H_\mathrm{M}=(n_1H_1+n_2H_2)-(n_1H_1^*+n_2H_2^*)$$

Using the excess enthalpies defined by

$$h_\mathrm{i}=H_\mathrm{i}-H_\mathrm{i}^*$$

and using the molar fractions:

$$\Delta H_\mathrm{M}=\frac{n_1h_1+n_2h_2}{n_1+n_2}=x_1h_1+x_2h_2$$

In a drop, after all corrections, the Joule measurement divided by the drops molar quantity (n_1+n_2) relates the molar mixing enthalpy ΔH_M. In continuous flow measurements and in steady state conditions, the molar rate is defined by

$$\frac{\mathrm{d}n}{\mathrm{d}t}=\frac{\mathrm{d}n_1}{\mathrm{d}t}+\frac{\mathrm{d}n_2}{\mathrm{d}t}$$

After the corrections, the measured power W (endothermic: >0) directly relates the enthalpy change by:

$$W(\mathrm{d}n/\mathrm{d}t)=\Delta H_\mathrm{M}$$

Conclusions

The chip heater produces practically constant values independent of the samples and/or working chambers. The manufacturers heater furnishes reproducible results but, also, a roughly information on energetic measurements. Appropriate corrections are necessary if accurate results are obtained.

The device sensitivity changes with the position in the available surface and, also, the heat losses to surroundings induces remarkable changes with the *z*-position. If the heat production is considered homogeneous inside the reaction chamber, measurement using Joule effects in several resistance permit and evaluation of the shape factor (*SF*) modifying the manufacturers sensitivity.

Under the hypothesis of a homogeneous heat dissipation the shape factor (*SF*) for each liquid (or mixture) can be approached by the ratio between the sensitivity in the middle of the chamber (*z*-position) *vs*. the sensitivity obtained from the chip resistance.

As a general approach for continuous flow mixtures, the relative steady state signal or signal divided by volume rate as μV min^{-1} need to be extrapolated to zero volume rate from high volume rates. The extrapolation avoids the parasitic effects at low volume rates related to initial mixture effects in the inlet tubing. The extrapolated value can be converted in W min μL^{-1} (J μL^{-1}) using the appropriate chip Joule sensitivity (divided by the *SF*).

The approaching method seems a reasonable approach to the thermodynamic values: the obtained values of enthalpies remains inside a bar of ±5%. Can be considered a roughly approach but traceable to Joule references. The results based on the chip heater differs from the thermodynamic values in a 10 to 20%.

The work is carried out in the frame of a cooperative program centered on the accuracy of conduction calorimeters and derived devices. The integrated actions HA 1999-0087 (MCT-Spain) and 314-Al-e-dr (DAAD, Germany) between Freiberg and Barcelona group are acknowledged. The ACES 1999-00040 (Gen. of Catalonia) related to 'nanocalorimeters' is gratefully acknowledged.

References

1 J. Lerchner, D. Caspary and G. Wolf, Sens. Actuators B, 70 (2000) 57.
2 Adaptronics and Smart Structures, H. Janocha Ed., Springer Verlag, Berlin FRG 1999.
3 Liquid nano calorimeter by Xensor Integration, Delft, The Netherlands (website: www.xensor.n1).
4 J. Lerchner, A. Wolf and G. Wolf, J. Therm. Anal. Cal., 57 (1999) 241.
5 J. Lerchner, A. Wolf, A. Weber, R. Hüttl and G. Wolf, in 'Microreaction Technology, Industrial Propects', Ed. W. Ehrfeld, Springer 2000, p. 469.
6 A. Wolf, A. Weber, R. Hüttl, J. Lerchner and G. Wolf, Thermochim. Acta, 337 (1999) 27.
7 D. Caspary, M. Schröpfer, J. Lerchner and G. Wolf, Thermochim. Acta, 337 (1999) 19.
8 C. Auguet, J. Lerchner, F. Martorell, F. Moll, H. Tachoire and V. Torra, 'Theoretical and Experimental Approach to 'nano-sized' Calorimetric Devices', Proc. of the Workshop on Trends on Shape Memory Behavior, Barcelona, pp. C-II-1-1 to C-II-1-4, April 3-4, 2001, Ed. V. Torra. CIRG-DFA-ETSECCPB-UPC, 2001.
9 C. Auguet, F. Martorell, F. Moll and V. Torra, J. Therm. Anal. Cal., 70 (2002) 277.
10 P. Dantzer and P. Millet, Thermochim. Acta, 370 (2001) 1.
11 V. Torra, C. Auguet, H. Tachoire, P. Marinelli and J. Lerchner, J. Therm. Anal. Cal., 66 (2001) 255.
12 J. L. Macqueron, J. Navarro and V. Torra, An. Fis., 73 (1977) 163.
13 E. Cesari, J. Hatt, E. Margas, J. Navarro, V. Torra, E. Utzig and W. Zielenkiewicz, Bull. Acad. Polon. Sci. Sér. Sci. Chim., 28 (1980) 297.
14 A. Isalgue, J. Ortin, V. Torra and J. Viñals, An. Fis., 76 (1980) 192.
15 V. Torra and H. Tachoire, J. Thermal Anal., 52 (1998) 663.
16 J. Lerchner, G. Wolf, C. Auguet and V. Torra, Thermochim. Acta, in press.
17 A. Wolf, Unpublished results (2000).
18 L. E. Briggner and I. Wadsö, J. Biochem. Biophys. Methods, 22 (1991) 101.